Article

Journal of the Brazilian Chemical Society

https://dx.doi.org/10.21577/0103-5053.20240019

J. Braz. Chem. Soc. **2024**, *35*, 7, e-20240019, 1-16

Stealth Behavior of Poly(ethyloxazoline)s-Modified Hydroxyethyl Starch-Based Nanocapsules

Lillian M. U. D. Fechine,[a,b] Biao Kang,[b] Susanne Schöttler,[b] Denise R. Moreira,[a,b] Danilo C. Queiroz,[a] Frederik R. Wurm,[b] Katharina Landfester[b] and Nágila M. P. S. Ricardo *,[a]

[a]*Departamento de Química Orgânica e Inorgânica, Universidade Federal do Ceará (UFC), Campus do Pici, 60451-970 Fortaleza-CE, Brazil*

[b]*Max Planck Institute for Polymer Research, Ackermannweg 10, 55128 Mainz, Germany*

Poly(oxazoline)s (POZs) are a "new" class of biocompatible polymers that show unique and specific properties for modern biomedical and biomaterials design applications. In this work, POZs-coupled hydroxyethyl starch nanocapsules were developed in order to create a powerful protein suppressor vehicle. Herein, POZs of different molecular weights were used to functionalize the well-known hydroxyethyl starch nanocapsules (HES) surface by metal-free "click" chemistry, in which HES have also been related to immune suppressor property. For each modification step, the capsules were characterized regarding size, morphology and charge surface, and, as expected, the "click" strategy kept a core-shell structure with an average diameter distribution < 200 nm. Additionally, previous to the post-polymerization modification step, the amount of free amino groups was determined by fluorescence intensity, allowing further "click" coupling of the surface of the capsules with POZs, later confirmed by gel permeation chromatography. Protein corona evaluation and aggregation assays in human plasma showed lower protein attaching for POZ-modified HES nanocapsules, than HES modified with polyethylene glycol ("PEGylated"-HES) and unmodified HES. Indeed, around 35% of "hard" protein corona of POZ-modified HES are clusterins, the apolipoprotein that can reduce the non-specific cellular uptake into macrophages, indicating that POZs have stealth behavior similar to polyethylene glycol (PEG), being a potential alternative to "PEGylated"-based nanocarriers.

Keywords: protein suppressor, poly(ethyl oxazoline)s, hydroxyethyl starch, nanocapsules, stealth effect

Introduction

The therapeutic performance of drugs is dependent on the physiological system within the human body, where physical, chemical, and biological barriers must be overcome to reach the target site. Once in the bloodstream, our immune system recognizes foreign molecules/materials and creates a complex and sophisticated network based on protein interactions, pH, temperature, charge, and concentration differences to rapidly remove these unknown materials from our bodies. Certainly, the drug/physiology relationship guides an infinite number of protein interactions that play a significant role in cellular uptake.[1,2] Therefore, the development of materials with stealth behavior, i.e., an effect related to protein corona suppression on particle surfaces, is crucial to prevent recognition by the immune system and thus avoid elimination from the organism, ensuring that the material can successfully achieve its therapeutic objective.

Synthetic and natural polymers have been extensively studied as the main source for development of various drug delivery systems with optimal response to body stimuli. These polymers can effectively shield both the carrier devices and the water-soluble drugs incorporated therein.[3-8] In the polymer-applied research field, polyethylene glycol (PEG) and hydroxyethyl starch have had great success in reducing cellular uptake in macrophage cells. They can reduce non-specific protein adsorption and selectively target a specific protein so-called clusterin, which has recently been discovered to be the major contributor to the "stealth" effect against immune system cells.[7-11]

For example, the natural polymer starch, a mixture of linear poly(1,4-ß-*D*-glucopyranose) and branched poly(1,4-ß-D-glucopyranose and 1,6-*D*-glucopyranose),

*e-mail: naricard@ufc.br
Editor handled this article: Célia M. Ronconi (Associate)

has enormous potential for biomedical applications, mainly due to its biocompatibility and biodegradability. However, especially for *in vivo* applications, native starch may not be suitable as it degrades rapidly and, in the case of a drug delivery device, may release the drug too quickly. On the other hand, hydroxyethyl starch is a less rapidly degraded derivative in which the C2 and C6 positions of each glucose unit are functionalized with a hydroxyethyl group. These additional groups slow down enzymatic degradation compared to natural starch, while maintaining biocompatibility.

Although their most common clinical use is in the treatment of hypovolemic shock, Landfester and co-workers[8] investigated hydroxyethyl starch (HES) nanocapsules as a drug delivery system with the possibility of post-surface modification. As expected, these nanocapsules showed excellent results, suppressing non-specific cellular uptake and prolonging blood circulation time.

In the case of PEG-based delivery systems, PEG is considered the "gold standard" due to its unique properties, such as increased water solubility, biocompatibility, and blood circulation time, as well as reduced renal clearance and immune recognition.[8,12-15] However, researches have shown that PEG is only partially biodegradable and can accumulate in certain organs. For example, PEG antibodies have been identified in patients treated with PEG-conjugated drugs, leading to a decrease in therapeutic efficacy.[16-18] In addition to the controversies associated with these limitations, they show that degradation and biodistribution of PEG are not yet understood, which poses clinical and commercial challenges for pharmaceutical companies.[16,19] Therefore, polymer science has been forced to overcome these limitations through new technological strategies, creating a certain need for PEG alternatives with similar or even better properties. This need is the main motivation for our research.

Poly(oxazoline) (POZ) is a relatively "new" class of synthetic polymers that has attracted increasing attention in biomedical applications, serving as a promising alternative to PEG overuse.[20-22] Among its numerous properties, POZs are pseudopeptides that are stable at room temperature and water-organic soluble, resulting in a biocompatible polymer.[19,22-25] Another relevant point is the similar "stealth" property as PEG, and it also showed no accumulation in human body tissues.[16,19,20] A well-defined POZ can be obtained by modulating the chain ends and side chains by cationic ring-opening polymerization (CROP). This has led to a wide range of POZ-based materials being investigated, opening up new possibilities for biomedical polymer applications. These include: (*i*) *in vivo* studies demonstrating rapid clearance from the body with no significant accumulation in organs and tissues; (*ii*) evidence of suppression of protein uptake and recognition by the reticular endothelial system (RES); and (*iii*) success in human blood compatibility.[19,25]

Furthermore, POZ-based drug conjugates and POZ-functionalized drug nanocarriers have been shown to have similar and/or even better advantages when compared to "PEGylated" materials.[20,26] However, a deeper knowledge of protein interactions and their "stealth" properties, along with the correlation of these properties as an intrinsic nature of the POZ polymer itself, has not been reported to date, leaving gaps in the influence and efficiency of the polymer in the biological environment. In addition, different types of POZ polymers, such as poly(ethyl oxazoline) (PetOx), have been developed to overcome the detection by the phagocytic cells as foreign entities in the body, enabling better therapeutic performance and drug delivery properties of these systems.[27]

This work proposes to develop an alternative route within the smart Drug Delivery System (DDS) challenge. It combines different synthesis strategies, where the miniemulsion technique has been chosen due to its outstanding synthesis performance, generating nanoscale capsules. This technique offers numerous possibilities for surface functionalization and efficient encapsulation of payloads.[3-5,28,29]

In this study, we synthesized a hydroxyethyl starch-based nanocapsule using a well-established method previously reported by Kang *et al.*[8] We used cooper-free "click" chemistry to functionalize the HES surface to further PetOx modification via a stable and selective triazole moiety.[7,30-33] To evaluate and compare the performance of PetOx-modified and unmodified HES nanocapsules, we investigated their size and stability in physiological media, as well as their stealth behavior *in vitro* assays. These assays included light scattering in plasma and protein corona analysis by sodium dodecyl-sulfate polyacrylamide gel electrophoresis (SDS-PAGE) and liquid chromatography-mass spectrometry (LC-MS). We believe that further advances in this relatively new area of research will contribute to the development of POZ-based platforms that fully exploit the versatility of this interesting class of polymers.

Experimental

Materials

The methoxy-PEG-azide (2.000 g mol^{-1}) was purchased from Sigma-Aldrich (Mainz, Germany), and also the organic crosslinker 2,4-toluene diisocyanate (TDI, 174.2 g mol^{-1}, Figure 1d) and cyclohexane (> 99.9%). Azide end-

functionalized poly(ethyl oxazoline)s ($PetOxN_3$) were kindly donated by the Jena University in Germany, and were synthesized from 2-ethyloxazoline monomers using the CROP reaction and terminated with an azide functional group. They consist of PetOx blocks with different molecular weights (2, 5 and 6 kDa). Details can be found in Table 1, and ^{1}H nuclear magnetic resonance (NMR) spectra are available in the Supplementary Information (SI) section (Figure S1).

Hydroxyethyl starch solution (20% m/v) was donated by Fresenius Kabi, Bad Homburg vor der Höhe, Germany (20.000 g mol^{-1}). Dimethyl sulfoxide (DMSO, > 99%) was purchased from Acros Organics (Mainz, Germany). The hydrophilic fluorescent dye sulforhodamine 101 (SR101) (606.71 g mol^{-1}) was acquired from BioChemica, Aldrich (Mainz, Germany) (Figure 1a). Phosphate buffer saline at pH 7.4 (PBS buffer) was purchased from Gibco (Mainz, Germany). The "click" chemical dibenzylcyclooctyne-NHS ester (DBCO) (478.50 g mol^{-1}) was obtained from Jena Bioscience GmbH (Jena, Germany) (Figure 1e). Boric buffer (1 M, pH 9.5) was prepared by standard guidelines by dissolving boric acid (B6768 Sigma, Mainz, Germany) in water and adjusting the pH using a 1% sodium hydroxide solution (NaOH, Sigma, Mainz, Germany). The anionic surfactant sodium dodecylsulfate (SDS) was purchased from Fluka in Mainz, Germany (Figure 1b). The oil-soluble surfactant polyglicerol polyricinoleate (PGPR) (Grinsted PGPR 90) was purchased from Danisco (Copenhagen, Denmark) (Figure 1c). For the purification process, Amicon® Ultra centrifugal filter tubes with a nominal molecular weight limit (NMWL) of 100.000 were purchased from Merck Millipore, in Mainz, Germany.

For *in vitro* assays, human citrate blood plasma was taken from healthy donors at the Department of Transfusion Medicine at the University Medical Center Mainz after physical examination and after obtaining written informed consent in accordance with the Declaration of Helsinki. The blood plasma of 10 healthy donors was pooled and stored at –20 °C. The study was approved by the local ethics committee "Landesärztekammer Rheinland-Pfalz" (Bearbeitungsnummer: 837.439.12 (8540-F)). Standard procedures for protein corona analysis were followed, using the Coomassie Brilliant Blue staining solution protocol for identification and Pierce 660 nm protein (Thermo Scientific, Rockford, USA) for quantifying the adsorbed proteins on the capsule surfaces. Milli-Q water and high-grade analytical reagents, as received, were used for all experiments.

Table 1. Molecular characterization of azide end-functionalized poly(ethyloxazoline)s, regarding molecular weight (M_w) by ^{1}H NMR

	$DP_{theorical}$ [a]	DP_{NMR} [b]	$M_{w\ NMP}$ [b] / (g mol^{-1})	PDI
$PetOxN_3$ 2 kDa	20	22	2.200	1.11
$PetOxN_3$ 5 kDa	50	53	5.300	1.09
$PetOxN_3$ 6 kDa	60	64	6.400	1.09

[a]According to the [M]/[I] ratio; [b]^{1}H NMR (300 MHz, $CDCl_3$). DP: degree of polymerization; PDI: polydispersity index.

HES nanocapsules synthesis

HES nanocapsules were prepared in an inverse miniemulsion system (water-in-oil) adapted from

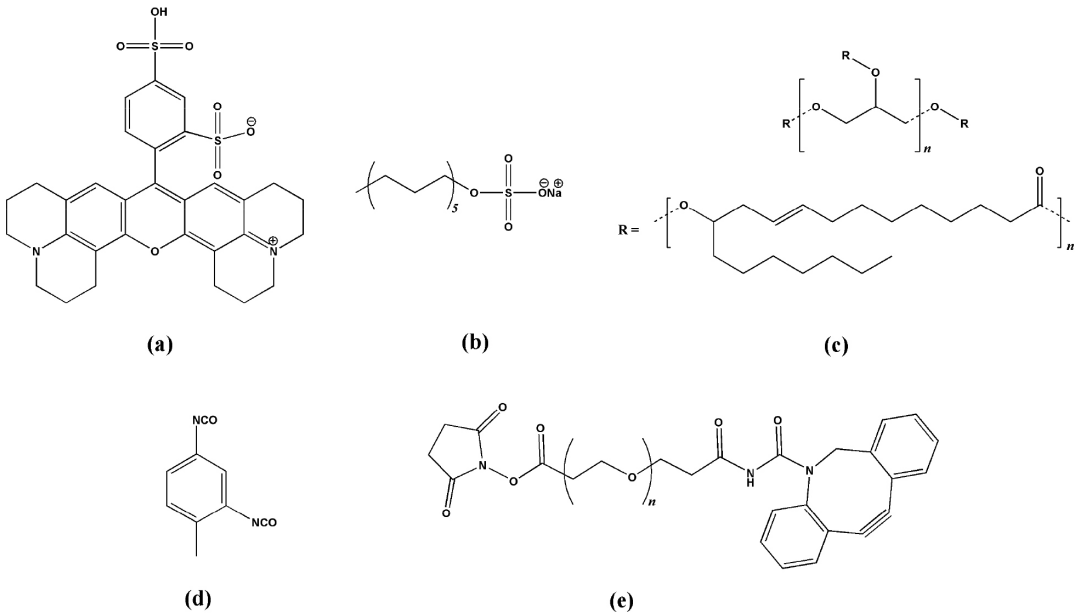

Figure 1. Chemical structure: (a) SR 101 fluorescent dye; (b) SDS surfactant; (c) hydrophobic PGPR surfactant; (d) crosslinker TDI and (e) dibenzylcyclooctyne-NHS ester.

previously published[8] protocols (Figure S2, SI section). The oil phase (OP) was prepared by dissolving 160 mg of PGPR in 14.5 g of cyclohexane and separated in three different flasks (OP1 = 7.5 g; OP2 = 5.0 g and OP3 = 2 g). The aqueous phase consists of 50 mg of SR101 (standard hydrophilic dye as a model for a low molecular weight drug) and 500 mg of standard HES solution (0.1 g mL^{-1}). Briefly, the aqueous phase was mixed with OP1 at 1000 rpm for 30 min, followed by ultrasonication at 70% amplitude for 3 min, with a pulse-regime of 20 s on and 10 s off, using a Branson Sonifier W-450-Digital (Massachusetts, United States) and a ½" tip. Then, OP2 was mixed with the dispersed solution, following the OP1 procedure. 50 mg of TDI were added into OP3, and dropwised into the final formulated miniemulsion. The interfacial crosslink reaction was carried out at 25 °C for 24 h. 1 mL of the nanocapsule dispersion in cyclohexane was purified by centrifuge at 4000 rpm for 30 min, in order to remove the excess of PGPR, and the precipitate was redispersed in 400 μL of fresh cyclohexane by pipetting up and down. Afterwards, in a sonication bath (Bandelin Sonorex, type RK 52H, Berlin, Germany), the purified nanocapsule dispersion in cyclohexane was added slowly into 5 mL of 0.1 wt.% SDS solution. After stirring overnight under 1000 rpm at room temperature to allow evaporation of cyclohexane, the SDS excess in the obtained nanocapsule dispersion was ultrafiltered using Amicon® centrifugal filter (Ultra-0.5, Ultracel-100 Membrane, 100 kDa) and used for standard characterizations by dynamic light scattering (DLS), ξ-potential, transmission electron microscopy (TEM) and scanning electron microscopy (SEM). Moreover, the whole standard characterizations made to unmodified HES capsules were also used to characterize the modified ones.

Determination of free amino groups

Prior to post-polymerization modification step, the amount of free amino groups at the surface of the nanocapsules was determined by the standard fluorescamine assay.[34] Preliminary, a standard hexylamine solution was used as a reference to establish a working function, fluorescence intensity *versus* fluorescamine-attached amino groups (mol L^{-1}), by aid of an Infinite M1000 plate reader from Tecan, Austria using 96-well at 25 °C by excitation at 410 nm and emission at 470 nm. A stock solution was prepared, mixing 2 mg of fluorescamine and 1.5 mL of anhydrous acetone. For the quantification procedure was added into Eppendorf tube 25 μL of the aqueous nanocapsule dispersion, around 0.2% of solid content (SC) previously determined, 725 μL of boric buffer (pH 9.5), followed by the addition of 200 μL of the fluorescamine stock solution. Then, the mixture was rapidly vortexed (Heidolph REAX2000, Schwabach, Germany) for 20 s, at maximum speed, and the fluorescence intensity was measured and quantified by aid of hexylamine calibration curve (Figure S3, SI section). All fluorescence measurements were made in triplicate.

Polymer modification on the HES nanocapsules

The polymer modification on the HES nanocapsule surface is based on the "click" reaction of the DBCO-coupled HES with the azido end-functionalized polymer to form a stable triazole. This method requires two-step reaction:

Step 1

A stock solution of DBCO was prepared, 1 mg L^{-1} in DMSO (storage at 4 °C). For the typical DBCO-activation on HES nanocapsule surface, to 1 mL of aqueous HES dispersion (adjusted pH 7.4 with PBS buffer) were added 300 μL of the DBCO stock solution. The reaction was carried out for 4 h at room temperature, and the unreacted linker was removed by ultrafiltration (Amicon® centrifuge units).

Previously the step 2, the amount of covalently DBCO coupled on HES surface was determined following standard method of azide-functionalized anthracene (AnN_3). Firstly, considering that all free $–NH_2$ groups on HES surface were DBCO-coupled, AnN_3 was added into 50 μL of HES solution (3:1 AnN_3: $–NH_2$, molar ratio) sample, subsequently, a certain DMSO volume was added until 100 μL. Besides, a blank, AnN_3 and DMSO, and a sample blank, 50 μL of HES solution and DMSO, were prepared according to the sample. After stirring overnight under light protection, fluorescence intensity measurements were obtaining using Infinite M1000 plate reader from Tecan, Austria using 96-well at 25 °C by excitation at 370 nm and emission at 414 nm. All fluorescence measurements were made in triplicate.

Step 2

The stable triazole moiety or "click" was formed when azide end-functionalized polymer ($PEGN_3$ and $PetOxN_3$ 2, 5 and 6 kDa) was added into 1 mL of aqueous DBCO-activated HES dispersion (3:1 polymer:DBCO, molar ratio) to produce HES-PEG and HES-PetOx 2, 5 and 6 K samples respectively. The reaction was allowed to proceed overnight under mild conditions at room temperature, and the unreacted polymer chains were removed by ultrafiltration (Amicon® centrifuge units) afterwards. Additionally, a well-known volume from PetOx

and PEG-modified HES capsules solutions were dialyzed during one week with Milli-Q water, to remove all non-covalent binding of polymer chains on HES surface.

After step 2, the qualitative determination of covalently "clicked" polymers on HES surface was measured by gel permeation chromatography (GPC). Purified unmodified HES nanocapsules dispersed in Milli-Q water, and SDS and pure polymers were analyzed as a positive and negative control, respectively. Moreover, alongside standard characterizations, polymer-modified HES nanocapsules, HES-PEG (positive control), HES-PetOx 2, 5 and 6 K, were investigated regarding protein adsorption and aggregation by *in vitro* assays, and protein corona composition.

Stealth behavior evaluation

Protein adsorption

Firstly, nanocapsule dispersions were diluted in 300 µL of Milli-Q water to a total capsule surface area of 0.05 m^2 and added into 1 mL of human plasma, after incubation for 1 h at 37 °C and stirring at 300 rpm to form aggregates, the nanocapsules were collected by centrifugation. After protein adsorption, the supernatant was removed, and the capsules were washed three times with 1 mL of PBS buffer by centrifugation at 4 °C for 1 h (20.000 g). In the protein desorption step, the nanocapsules were resuspended in 300 µL of 7 M urea/2 M thiourea/4% CHAPS buffer, incubated for 15 min at 37 °C, 600 rpm, and pelleted again by centrifugation. Then, the supernatant was collected into a fresh low-bind tube and used for protein quantification using the standard assay Pierce 660 nm protein by plate reader.

For protein identification, the SDS polyacrylamide gel electrophoresis (SDS-PAGE) method was used. For SDS-PAGE, 16.25 µL of the collected protein sample were mixed with 6.25 µL NuPAGE LDS sample buffer and 2.5 µL NuPAGE sample reducing agent. Then, the mixture was applied onto a NuPAGE 10% Bis-Tris Protein Gel (Novex, Thermo Fisher Scientific, Waltham, USA). The electrophoresis was carried out in NuPAGE MES SDS Running Buffer at 150 V for 1.5 h with SeeBlue Plus2 Pre-Stained Standard (Invitrogen, Carlsbad, CA, USA) as a molecular marker. The gel was stained using Coomassie Brilliant Blue R-250 staining solution (Novex, Thermo Fisher Scientific, Waltham, USA). For centrifugation, the Sigma 3 k-30 from Sigma Centrifuges, UK, was used. For quantification procedure, the bovine serum albumin (BSA) was used as a standard protein. The samples were stored at −80 °C until needed for further experiments, and all measurements were made in triplicate.

Aggregation behavior by light scattering (LS) in plasma

The aggregation behavior was investigated following a well-established protocol, firstly published by Rausch *et al.*[35] All modified and unmodified HES nanocapsules measurements were made in PBS buffer at mimicked physiological pH (7.4) and salinity (0.152 M). For nanocapsules/plasma mixtures, 10 µL of nanocapsules (NCs) dispersion (around 0.2%) were added into the light scattering (LS) cuvette containing 200 µL of human plasma. After filtered into the cuvette using a GS200 nm filter, the mixture was diluted to 1 mL total volume by PBS (filtered) into the LS cuvette. For the nanocapsule blank, 10 µL of the NCs dispersion were added into 990 µL of PBS. Similarly, the blank was prepared adding 200 µL of plasma into 800 µL of PBS, maintaining the same dilution proportion. Previously the measurements, the samples were incubated on a shaker during 20 min at 37 °C, in which LS measurements were also performed at 37 °C.[35]

Protein corona composition

Briefly, proteins were digested following the well-established protocol: 25 µg of each collected protein sample were precipitated and added trypsin with 1:50 ratio (enzyme:protein).[36] For LC-MS analysis, the samples were diluted (10-fold) with aqueous 0.1% formic acid and spiked with 50 fmol μL^{-1} Hi3 EColi Standard (Waters Corporation, Massachusetts, USA) for absolute quantification.

The LC-MS was performed using a nanoACQUITY UPLC system coupled with a Synapt G2-Si mass spectrometer (Waters Corporation, Massachusetts, USA). Tryptic peptides were separated on the nanoACQUITY system equipped with a C-18 analytical reversed-phase column (1.7 µm, 75 µm × 150 mm, Waters Corporation) and a C-18 nanoACQUITY Trap Column (5 µm, 180 µm × 20 mm, Waters Corporation). Samples were processed with two different mobile phases: A, consisting of 0.1% (v/v) formic acid in water, and B, acetonitrile with 0.1% (v/v) formic acid. As a reference compound 150 fmol μL^{-1} Glu- Fibrinopeptide were infused at a flow rate of 0.5 µL min^{-1}. Electrospray ionization was performed in positive ion mode using a NanoLockSpray source. Data was acquired over a range of *m/z* 50-2.000 Da with a scan time of 1 s, ramped trap collision energy from 20 to 40 V with a total acquisition time of 90 min. All samples were analyzed in duplicate. Data acquisition and processing was carried out using MassLynx 4.1 and TansOmics Informatics software to process data and identify peptides. The generated peptide masses were searched against a reviewed human protein sequence database downloaded from Uniprot. Quantitative data were generated based on the TOP3/Hi3 approach, providing the amount of each protein in fmol.

Standard characterizations

The average size of the capsules was measured by dynamic light scattering (DLS) using a PSS Nicomp Particle Sizer 380 (Santa Barbara, CA, USA). The capsule dispersion was diluted ca. 10× by Milli-Q water. The scattered light was detected at 90°, while the temperature was maintained at 25 °C.

The zeta potential of capsules was measured by diluting to a solid content of 10^{-9}% by Milli-Q water in a Zeta Sizer Nano Series (Malvern Instruments, UK) at 25 °C.

SEM measurements were carried out by using a LEO (Zeiss) 1530 Gemini device (Oberkochen, Germany). The samples were diluted to a solid content of 0.01% with Milli-Q water, where 15 mL of the diluted sample were placed on the silica wafer and dried at room temperature overnight. Transmission electron microscopy (TEM) measurements were carried out by using Jeol 1400 device at 80 kV (JEOL Company, Tokyo, Japan) accelerating voltage. The samples were diluted in the same way for SEM sample preparation. Then, 2 mL of the diluted sample were placed on a copper grid, which was covered by a 5 nm thick carbon film.

GPC measurements of unmodified and modified HES capsules were performed in *N*,*N*-dimethylformamide (DMF) with a flow rate of 1 mL min^{-1} using a PSS SecCurity Agilent Technologies 1260 Infinity instrument with an autosampler and a PSS GRAM 0.8 × 30 cm column at 60 °C with a particle size of 10 µm and pore sizes of 10.000, 1.000 and 100 Å. RI-detector G1362A RID was used for detection and poly(styrene) was used for calibration. Standard of the pure polymers, PetOx and PEG, and SDS were also analyzed as a negative control.

The polarity evaluation method was adapted from Viegas *et al.*[19] High performance liquid chromatography-reversal phase (HPLC-RP) measurements of $PEGN_3$ and $PetOxN_3$ polymers with different molecular weights (2, 4 and 22 kDa, and 2, 4 and 6 kDa, respectively) were performed using a C-8 column (15-20 µm particle size) and a gradient mobile phase (methanol/water, 0-5/5-100) with an ELSD-detector with UV detection.

Results and Discussion

HES nanocapsules synthesis and characterization

HES nanocapsules were prepared via inverse miniemulsion (water-in-cyclohexane). The core-shell structure is based on a crosslinker reaction using TDI by the nucleophilic addition of hydroxyl groups from HES to the electrophile isocyanate groups (–NCO) from TDI, which occurs in water-in-oil droplet interface.

As described in the Experimental section, HES and the hydrophilic fluorescent dye SR101, added to trace the cellular uptake in further studies, were dissolved in water and dispersed in the organic phase (OP1), forming nanodroplets by ultrasonication, and stabilized with PGPR surfactant. After dispersed in organic phase (OP2), TDI was slowly added to the miniemulsion, and the polyaddition of isocyanate to two monomers from HES formed the polysaccharide shell. Indeed, after the nanocapsules core-shell structure-formed, unreacted isocyanate groups from the crosslinker TDI on the surface of the capsules are hydrolyzed into primary amino groups during the subsequent redispersion step to aqueous phase. Later, these free amines are used as nucleophilic groups to enable a "click" reaction via DBCO with the azido end-functionalized $PetOxN_3$ on the surface of the capsules.

The encapsulation efficiency and permeability assays were not investigated in this work, as these results were published by Kang *et al.*[8] using the same HES-based synthesis method and model dye, showing that these nanocapsules were loaded with a high encapsulation efficiency of around 90% and exhibited a high density nanowall, even after one month of storage at room temperature.[8] As the standard protocol was strictly followed,[8] in this work, we only reproduced the characterization in terms of size by DLS, charge surface by ξ-potential (zeta potential) and morphology by SEM and TEM, as shown in Table 2 and Figure 2.

In Figure 2 is shown the morphology of the capsules, investigated by TEM and SEM. As expected from a conventional miniemulsion polyaddition reaction,[37] the interface polyaddition reaction synthesized spherical nanocapsules with a core-shell structure < 200 nm, in agreement with other works that used the same methodology.[3-5]

The solid content (SC / wt.%) is given by g of HES nanocapsules *per* g of HES solution ($g/g_{solution}$) or/and wt.%, where from each HES synthesis batch was determined by weighting HES nanocapsules solution and non-water-containing HES nanocapsules. The dispersed solutions had a solid content around 0.2 wt.%, which was expected considering previous purification steps, allowing further use for post-modification procedures.

The method of HES synthesis showed an efficient reproducibility with hydrodynamic radii of around 81.39 ± 0.81 nm, see Table 2. Comparing TEM and SEM images (Figure 2), the DLS values seem to be bigger, but the diameter still being < 200 nm. In this case, the hydration layer on HES surface must be considered, since the DLS measurements are in aqueous dispersion. The ξ-potential of the unmodified HES nanocapsules was

Table 2. Characterization of synthesized nanocapsules: unmodified HES and polymer-modified HES

	r / nm	ξ-potential / mV	Amino amount[a] / capsule	DBCO efficiency of conversion[b] / %
HES	81.39 ± 0.81	–40.5 ± 9.1	58,260 ± 4,950	–
HES-PEG	125.5 ± 1.23	–35.6 ± 12.8	–	60.28 ± 13.4
HES-PetOx 2K	83.8 ± 1.20	–35.0 ± 8.9	–	
HES-PetOx 5K	93.0 ± 1.32	–30.1 ± 10.0	–	
HES-PetOx 6K	77.6 ± 0.50	–32.0 ± 6.5	–	

[a]Considering for all calculation, based on Avogrado's constant: HES SC% of 0.26 ± 0.005 wt.%, radius and volume of the capsules in solution; [b]determined from AnN_3 assay, described in the Experimental section. *r:* hydrodynamic radius; ξ-potential: zeta potential; DBCO: dibenzylcyclooctyne-NHS ester. HES: hydroxyethyl starch nanocapsules; PEG: polyethylene glycol.

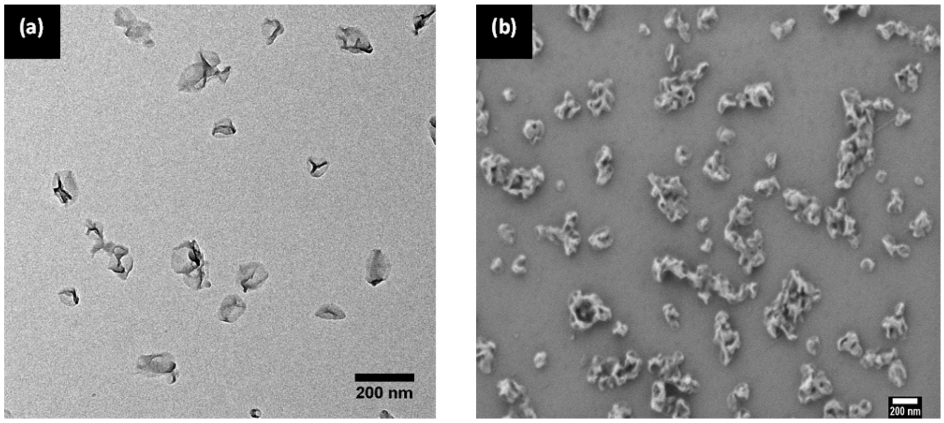

Figure 2. Images of synthesized HES nanocapsules: (a) TEM and (b) SEM.

negative, around –40 mV (Table 2), even with the positive charge contribution from free $–NH_2$ groups on HES surface. This can be explained due to the presence of remaining anionic SDS used for the redispersion process at 0.1 wt.% in aqueous solution, even after persistent dialysis for 7 days. This negative value also suggests nanocapsules stabilized by electrostatic repulsion acting as a hindrance barrier, preventing capsules from aggregating when dispersed on aqueous medium. Furthermore, the surface charge of a given nanocapsules species determines colloidal stability, governs protein adsorption, and, thus, may influence cellular uptake and aggregation under physiological medium.[38]

The number of amino groups on the surface of the nanocapsules was determined by standard fluorescamine assay, where the number of free amino groups *per* capsule can be determined. This standard method is adapted from the fluorometric assay of proteins, first reported by Böhlen *et al.*,[34] in 1973, in the sense of nonoscale quantification. Basically, the fluorescamine reacts with primary amino groups to yield highly fluorescent products. In this context, the fluorescence intensity obtained from fluorescamine-attached amino groups on HES capsules surface were measured and plotted in hexylamine calibration curve ($R^2 = 0.9982$), giving around 58,260 ± 4,950 primary amino groups *per* capsule (values are shown in Table 2). The high yield –NCO conversion to $–NH_2$ on HES surface was just observed due to the slightly higher amount of used TDI than the amount of reactive –OH groups in hydroxyethyl starch molecules, and therefore, the residual –NCO groups could be converted to free $–NH_2$ groups through hydrolysis. Further, as already mentioned, these free $–NH_2$ groups on HES surface were used for the covalent coupling polymer post-modification by "click" reaction via DBCO.

"Click" chemistry: $PetOxN_3$ to HES surface via DBCO

In this research, we have proposed POZ as a promising stealth polymer, offering an alternative to PEG. Our goal is to develop a robust drug delivery system with exceptional attributes by harnessing biodegradability and versatility of both HES capsules and PetOx polymer. Within this framework, our system is based on a synthetic pathway of DBCO-activated HES with the azide end-functionalized PetOx to form stable triazoles moieties on HES surface, giving covalently polymer-modified HES capsules (Figure 3).

PetOx-modified HES nanocapsules using different molecular weights of $PetOxN_3$ were prepared, HES-PetOx 2, 5 and 6 K, for further studies based on the correlation between hydrophobicity of the polymer and the suppressing protein adsorption, also the aggregation behavior in human plasma. Furthermore, PEGylated-HES nanocapsules (HES-PEG) were synthesized as a positive control in the stealth behavior investigation.

The DBCO-based cooper-free "click" chemistry reaction was applied as a strategy in this work due to bioorthogonal chemistry concept, in which the stable triazole is inert, not reacting in living systems, thereby not chemically interfering in any bioprocesses under physiologic environment. Furthermore, that "click" chemistry does not require a catalyst, since decreases the activation energy for the cycloaddition.[39] Chemically, the DBCO is a labeling compound acting as NHS ester-activated crosslinker that reacts with primary amine groups under mild conditions at physiologic to slightly alkaline medium (pH 7 to 9), in order to yield stable amide bonds, as seen in Figure 3a. Although this "click" reaction has been reported as a very fast pathway, resulting in chemoselective and stable triazoles, it is still necessary to know the efficiency of conversion or degree of functionalization, e.g., how many of these groups are actually converted to DBCO-activated moieties, enabling to participate of the latter $PetOxN_3$ and $PEGN_3$ attachment.

For DBCO-activated HES nanocapsules, a "click" reaction method using azide-functionalized anthracene (AnN_3) was performed for quantitative determination of the covalent bond of DBCO-NHS ester with primary amino groups on HES surface via amide bond. The efficiency of conversion is shown in Table 2. Generally, the "click" chemistry by DBCO shows great yield conversion, in this work it was observed 60.28 ± 13.4% of efficiency of conversion, e.g., not all primary amino groups on HES surface reacted with DBCO-NHS ester to form amide bonds, even under controlled reaction conditions,

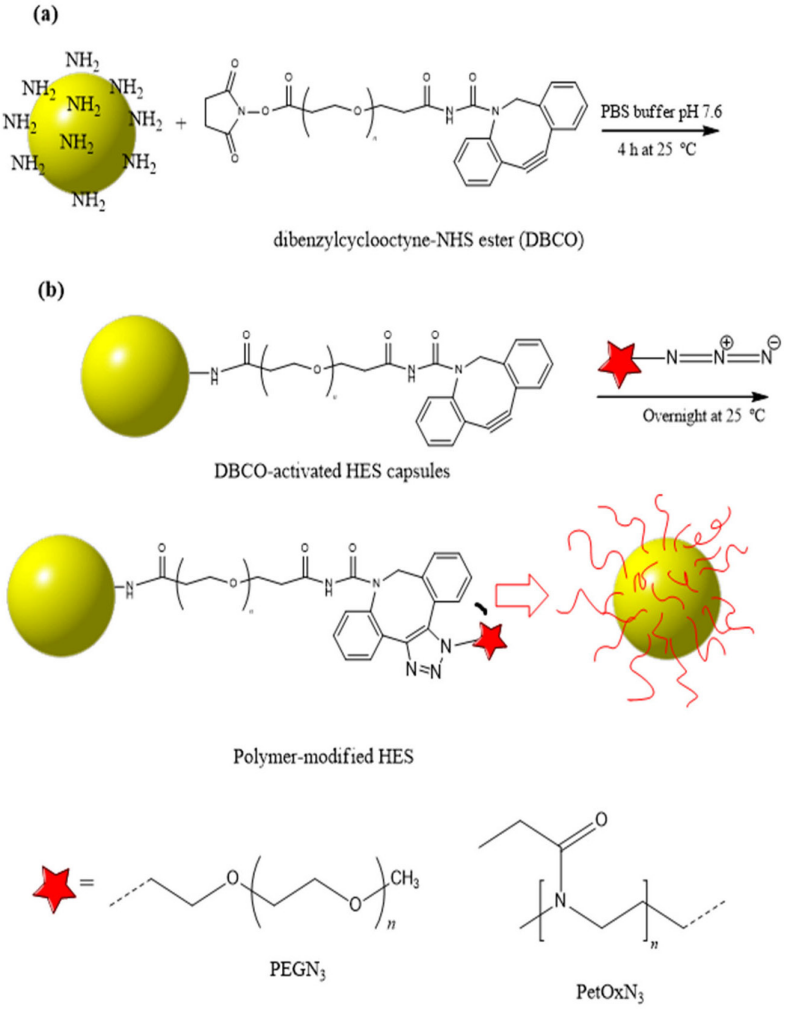

Figure 3. Synthetic pathway of functionalization steps on HES nanocapsules surface via DBCO "click" chemistry reactions: (a) DBCO-activated HES synthesis in PBS buffer; (b) polymer-modified HES coupling reaction in aqueous medium.

where some important steps were strictly followed, as described in product information sheet advises. Even though, that efficiency conversion ratio is great enough to allow the post-modification on HES surface by azide end-functionalized polymers.

Finally, the coupling of $PetOxN_3$ and $PEGN_3$ on the surface of the capsules was enabled to perform in aqueous dispersion, following the synthesis process described in the Experimental section, as shown in Figure 3b. After DBCO-activated HES synthesis, the dispersed nanocapsules solution was ultra-purified by Amicon® centrifuge units, removing unreacted and/or hydrolyzed DBCO molecules, and possibly by-products that may badly influence the polymer attachment reaction. The coupling reaction is shown in Figure 3b.

Briefly, the purified DBCO-activated HES nanocapsules solution was added into aqueous solution of azide end-labeled polymer at room temperature, where the strain-promoted cycloaddition began via nucleophilic addition in the C_{sp} of the cyclooctyne. Despite being chemoselective, 3 eq. of the polymer molecules were added to overcome steric effects by polymer chains. Then, after overnight reaction, unreacted azide end-labeled polymer chains were removed under ultra-purification process by Amicon® centrifuge units.

In Figure 4b is shown the average hydrodynamic radius and zeta potential values of HES-PetOx 2, 5 and 6 K. After coupling, the hydrodynamic radius of the capsules should increase slightly due to the presence of additional "clicked" molecules on HES surface, as observed for HES-PEG with average radius of 125.5 ± 1.23 nm, and also for Kang *et al*.,[8] who reported "PEGylated" HES nanocapsules. However, comparing to unmodified HES radius in aqueous dispersion with 81.39 ± 0.81 nm, a significant increase in size distribution was observed for the attachment with PetOx 5 K (93.0 ± 1.32 nm), and considering standard deviation, a slightly increase was also observed for HES-PetOx 2 K (83.8 ± 1.20 nm), and the opposite was noticed for HES-PetOx 6 K (77.6 ± 0.50 nm) instead. A further investigation was carried out through a comparative study by DLS in different angles. In Figure 4a is shown the comparative size evaluation by different angles, and as expected, the same behavior was noticed for all different analyzed angles, indicating that the hydrodynamic size is influenced by the hydration layer formed on capsule's shell, since it is measured in aqueous dispersion.

As a necessity, we evaluated a polarity comparative study between PetOxs and PEGs, concerning their molecular weight difference by reversal phase-high performance liquid chromatography (RP-HPLC), see Figure 4c. All elution volumes are shown in Figure S4 (SI section). As expected, PetOx polymers were more hydrophobic than PEGs in all analyzed molecular weights, suggesting that PetOx molecules should be less hydrated than PEG in aqueous medium.[19] Absolutely, the hydrophobicity is more evident when the molecular weight of the polymers increase. We found that this relative hydrophobic behavior may compensate the additional hydrodynamic radius size observed in DLS results, where the post-modification reaction with PetOx polymers decreased the hydrodynamic radius of the nanocapsules. Although, as a decrease was not notice for HES-PetOx 6 K, a further investigation about the polymer hydrophilic-lipophilic balance contribution should be done, in order to identify how that affects the colloidal properties of the capsules. All samples presented values of PDI around 0.1 and 0.4, being classified at moderate polydisperse nanocapsules, even after polymer-coupled reaction, and the difference between uncoupled HES was not considerable.

However, ξ-potential values after polymer-coupled reaction were slightly different compared to the unmodified HES capsules (Figure 4b). In general, the decrease of values should mainly depend on the charge of molecules that were "clicked" on HES surface, i.e., increasing the length of polymers the charge shielding is improved. For modified HES-PetOx 2, 5 and 6 K capsules, a slight decrease in the ξ-potential was observed, with negative values around −35.0 ± 8.9, −30.1 ± 10.0, and −32.0 ± 6.5 mV, respectively. These results indicate a significant amount of residual SDS after purification through dialysis. Furthermore, the additional non-charge PetOx molecules do not create a positive charge layer on HES capsules surface. In the case of HES-PEG, it was observed that there was no significant decrease in the ξ-potential, with a value of approximately −35.6 ± 12.8. However, this finding may suggest the attachment of the PetOx and PEG to the HES surface. This relative hydrophobic behavior may compensate the additional hydrodynamic radii size, observed in DLS results, from the "clicked" polymer decreasing the hydrodynamic radius of the nanocapsules. Although, as a decrease was not noticed for HES-PetOx 5 K, a further investigation about the polymer hydrophilic-lipophilic balance contribution should be done, in order to identify how that affects the colloidal properties of the capsules.

Controversially, a difference in size among PetOx-modified HES with different M_w was not observed compared to TEM images, as shown in Figure 4d, suggesting that even after PetOx attachment, the morphology of the capsule was not disturbed. As expected, the use of bioorthogonal chemistry such as azide strain-promoted cycloaddition did not cause any type of modification in the substrates including capsules surface.[39] Nevertheless, all PetOx-modified HES capsules showed smaller hydrodynamic radii compared to

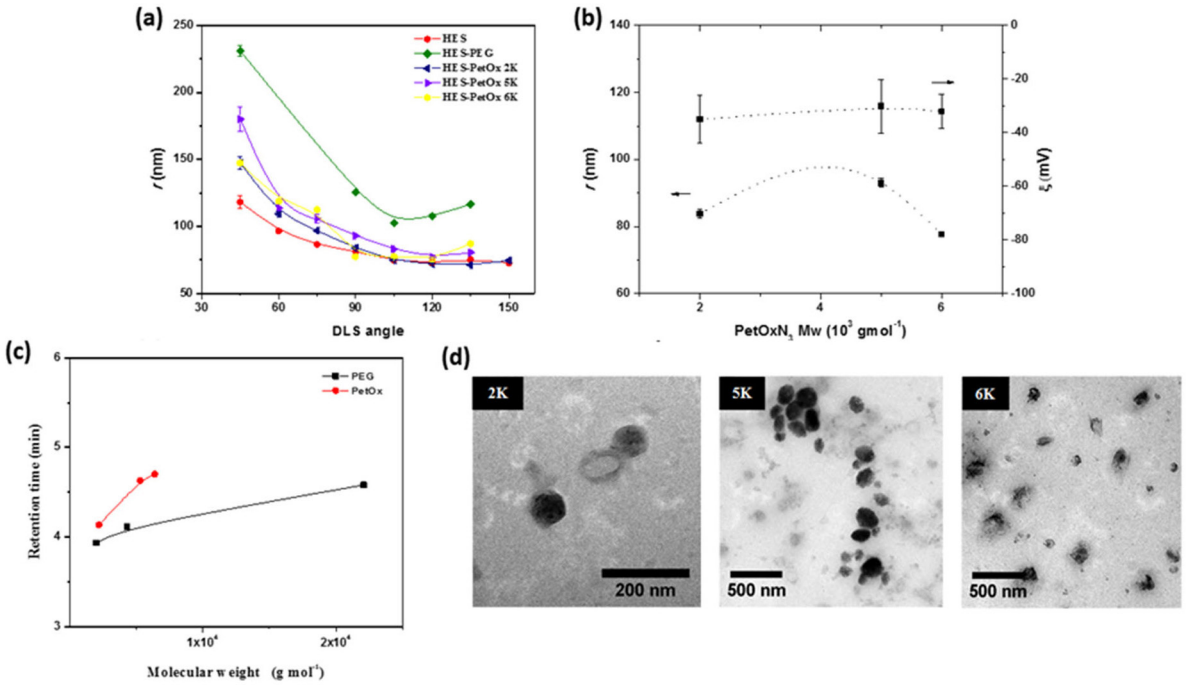

Figure 4. (a) Comparative investigation of hydrodynamic radius of HES, HES-PetOx 2, 5 and 6K, and HES-PEG by DLS with different angles; (b) hydrodynamic radii values at 90° (left) and zeta potential (right) of HES-PetOx 2, 5 and 6 K; (c) polarity comparative evaluation of pure polymers PEG (2, 4 and 22 kDa) and PetOx (2, 5 and 6 kDa) by RP-HPLC; and (d) TEM images of PetOx-modified HES: (2 K) HES-PetOx 2 K, (5 K) HES-PetOx 5 K and (6 K) HES-PetOx 6 K.

HES-PEG, potentially being an alternative to PEGylated capsules, as initially proposed.

Studies[10,13] have proved that physically adsorbed PEG-polymers-like can leave the surface coverage, making holes, where proteins can easily bind. Thereby, desorption can negatively affect the biodegradation of the capsule, increasing the loss of surface bound PEG.[40] Recently, Kang *et al*.[8] obtained success combining biodegradability of HES nanocapsules with the well-known PEG stealth properties by different methods of covalently coupling. *In vivo* tests have proved that the covalent effective "PEGylation" increased the plasma half-life time of the HES-PEG capsules. In this sense, some methods have been developed to investigate the covalent coupled polymer chains, as well as, to relate directly or/and indirectly the bounded polymer with the stealth behavior itself.[8]

In this situation, a substantiated proof for the covalently binding of the polymers on capsules' surface must be confirmed. Much efforts have been focused on ensuring this covalently attachment. However, there are instances when accurately quantifying the amount of attached polymer on nanocapsule's surface proves challenging. Furthermore, stablishing a direct link between the stealth effect and the resulting polymer layer presents its own set of complexities.

Therefore, an extensive purification process was taken before polymer qualitative determination. Even after ultrafiltration, a dialysis procedure was carried out at low temperature (ca. 4 °C) for HES-PetOx 2, 5 and 6 K nanocapsules, and for HES-PEG at room temperature, since the decrease of the temperature increases the hydration of azide end-poly(ethyl oxazoline)s chains, which becomes easier to remove both the physically adsorbed polymer on HES surface and the "free" unreacted polymer from the aqueous dispersion.[20] After several purification steps, coagulation of the nanocapsules was also observed, even initially the nanocapsules were redispersed in SDS 0.1% solution. As expected, the steric effect from the attached polymer does not compensate the static stabilization from the surfactant, which becomes too low under purification process. Surely, ultra-filtration and dialysis still been necessary, since for biological applications the use of surfactants should be avoided owing to their cytotoxicity.

GPC was found to be a suitable technique to identify possible physically adsorbed polymers on capsules' surface. After intense purification process by dialysis and ultrafiltration, all unreacted polymer chains should be gone. Finally, the qualitative efficiency of the "click" and the purification step were confirmed by GPC. In Figures 5a and 5b are shown GPC traces in DMF *vs.* PEG standards with RID detection for HES-PetOx 2 K and HES-PEG nanocapsules, purified unmodified HES as a positive control dispersed in Milli-Q water, and SDS and pure polymers as a negative control.

GPC traces showed a broad distribution for the pure polymers PetOx 2 K and PEG with peaks maximum of ca. 32.7 and 32.3 mL, respectively. After polymer attachment on HES, as any peak was detected in HES-PetOx 2 K and HES-PEG elugrams, a sustained proof that no polymer is physically adsorbed on HES surface can be rationalized. Indeed, elution volumes belonging to SDS surfactant were not observed for polymer coupling samples, also confirming the efficiency of the purification process, in which all unreacted polymer chains were removed in the dialysis for both PetOx and PEG polymers.

Stealth behavior evaluation

The nanoscience revolutionized many areas of medicine, developing small size materials with body-response properties. However, a deeper knowledge about the interaction of nanoscale materials in the body system is lacking. As well-known, once in the living system, the protein and other biological molecules present in the bloodstream form a protein corona on the nanocapsules surface, which opsonin proteins can bind to non-protected nanocapsules, allowing recognition by RES, and easily remove them from the body before the therapeutic performance.

PEG has been over-used as a "gold" standard in pharmaceutical formulations, since it can reduce these protein adsorptions promoting the stealth effect. Besides our group has published outstanding results concerning the stealth behavior of HES and PEG-modified nanoparticles/capsules,[8] some unlikely limitations have been reported regarding to PEG body accumulation. Thereby, still the challenge for searching alternative polymers with greater or similar stealth properties of PEG.

As the stealth effect of the capsules is mainly governed by the surface-formed protein corona, understanding the PetOx-modified HES behavior into biological fluids has become the main motivation of this work, investigating both the composition of protein corona and the nanocapsules aggregation, after human plasma incubation.

Aggregation in HB plasma

Even after size evaluation by DLS, controlling the size of the nanocapsules still being extremely necessary in order to avoid aggregates formation in the blood streaming that may negatively affect their biodistribution. In this work, we monitored the size distribution of nanocapsules in human plasma by a well-established light scattering protocol,[35] aiming the closest aggregation behavior evaluation into living systems.

As shown in Figure 6, the self-autocorrelation of the function capsules/plasma mixture is described by the force fit, which is kept fixed. It represents the sum of the correlation functions from each known plasma and nanocapsule parameter. If non aggregation is formed, the fit parameters consist only by the intensity contributions of NCs and plasma. If aggregates form, the fitting function is adjusted by adding another intensity contribution correlated to aggregate fit parameter.

For all samples, no aggregates larger than nanocapsules and plasma were found, except for HES and HES-PetOx 6 K, which can be observed by the perfect match between the correlation function of the HES-nanocapsules/plasma mixture and the sum of the correlation function from each increment.

For HES and HES-PetOx 6 K, a multicomponent intensity distribution was performed, indicating a slightly aggregation intensity value of 14.3 and 13.2% with r_h of 186.9 and 336.7 nm, respectively (Table 3). This aggregation formation may be related to a larger protein corona layer after human plasma incubation. For HES-PetOx 6 K, it can be assumed that the stealth effect may be suppressed by hydrophobicity increment of the PetOx 6 K, leading to increased protein uptake and consequently particle aggregation.

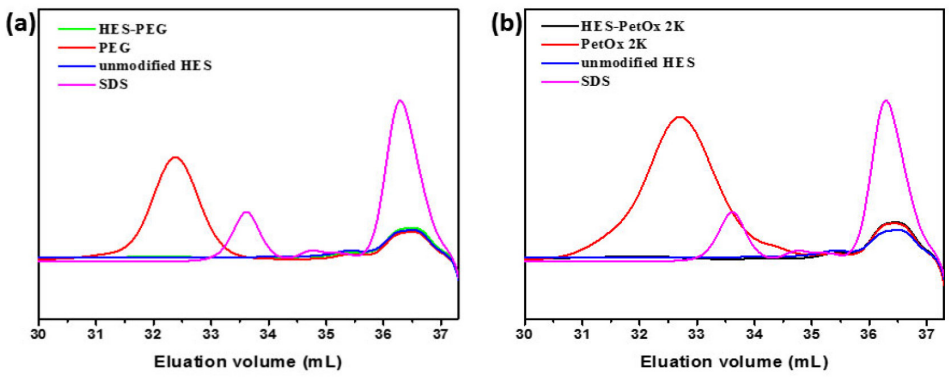

Figure 5. (a) HES-PEG and (b) HES-PetOx 2 K elugrams in DMF with RID detection, and their respective positive and negative controls.

Table 3. Hydrodynamic radius of all analyzed nanocapsules at 90° after human plasma incubation

	r_h[a] / nm
HES	83.7(186.9)[b]
HES-PEG	96.6
HES-PetOx 2 K	118.1
HES-PetOx 5 K	168.3
HES-PetOx 6 K	72.7 (336.7)[b]

[a]Hydrodynamic radius of the particle at 90º in water after human plasma incubation; [b]hydrodynamic radius of the aggregates at 90º in water after human plasma incubation. HES: hydroxyethyl starch nanocapsules; PEG: polyethylene glycol.

In the case of unmodified HES, this aggregation can be governed by the lower hindrance barrier of HES surface, in comparison to PetOx 2 and 5 K, which may increase protein uptake. Both results are supported by colloidal behavior of these samples, considering DLS discussion, and will be further evaluated by proteomic assay in the next section. Nevertheless, since no aggregation was detected for other samples, even after polymer attachment, the PetOx-modified HES samples maintained their lower diameter size in human plasma.

Protein adsorption

Evaluate and understand the protein adsorption, along with the composition of the protein corona on capsules when exposed to human plasma, represents the initial step to investigate the stealth behavior facilitated by the polymer-binding on HES surface.

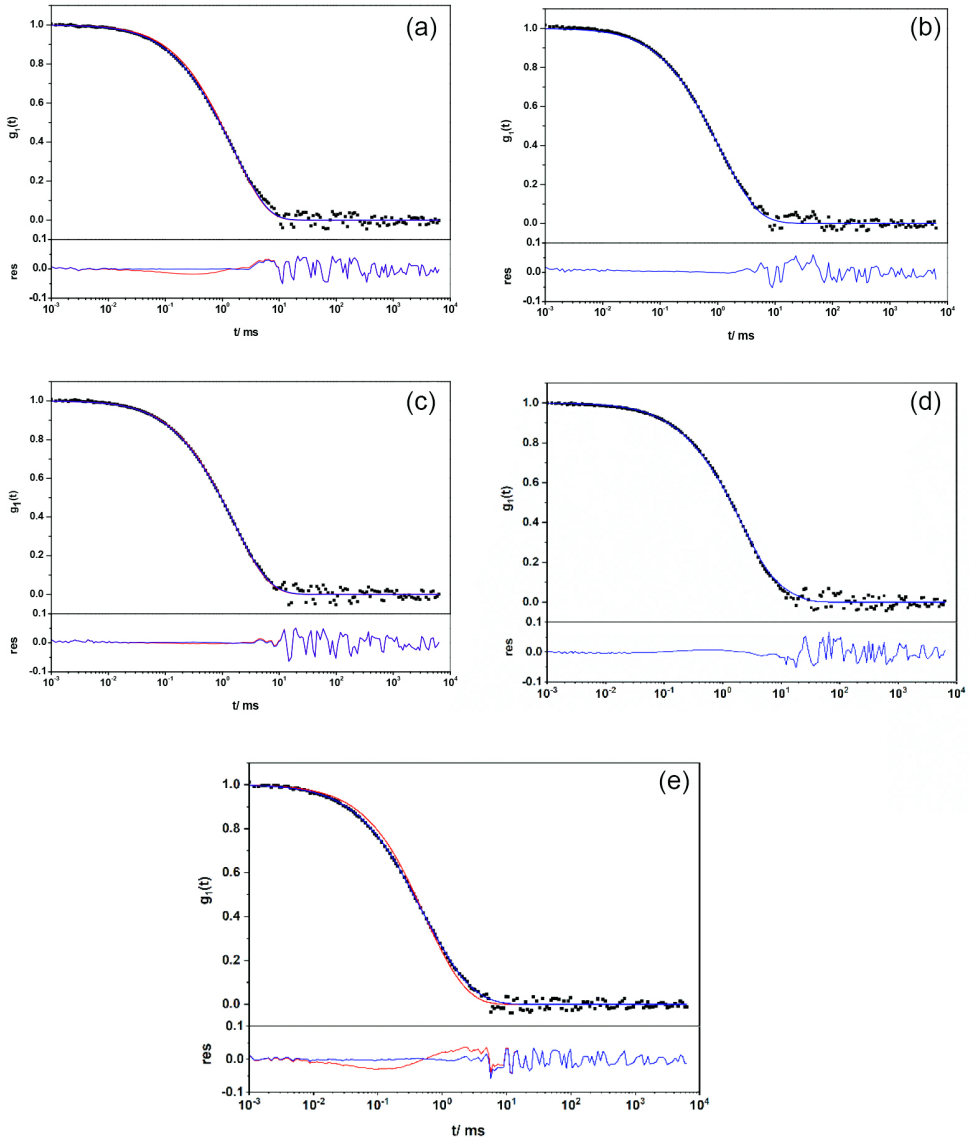

Figure 6. Self-autocorrelation functions of the HES-nanocapsules/plasma mixture, scattering angle: 60° at 37 °C: (a) HES, (b) HES-PEG, (c) HES-PetOx 2 K, (d) HES- PetOx 5 K and (e) HES- PetOx 6 K, where black squares are the data points of the mixture, and the red and blue curves represent the force fit of the mixture and the residue of the fit, respectively.

As described in the Experimental section, after incubation into human plasma, the proteins adsorbed on capsules surface HES, HES-PetOx and HES-PEG (positive control), were collected into a low-bind tube by centrifugation to be analyzed by SDS-PAGE procedure to protein visualization using Coomassie Brilliant Blue staining solution assay, and further quantified by standard assay Pierce 660 nm protein.

Gel electrophoresis technique has been extensively used in protein corona of nanocapsules/particles characterization under physiologic medium. Basically, this method determines the molecular weight of proteins through size exclusion using a defined pore size polyacrylamide gel under an electric field, promoting the migration of the SDS-charged proteins. The M_w can be determined by comparing a protein marker with known molecular weight of different proteins. Previously to SDS-PAGE procedure, the protein was stained with Coomassie Brilliant Blue dye, in which the dye binds to protein and is converted to a stable non-protonated blue form. In Figure 7b is shown the SDS-PAGE gel, where in the first left vertical line was applied the protein marker with standard M_w, the right subsequently lines show fractionated proteins from unmodified HES and polymer-modified HES, and the right line is the human plasma (HB plasma) used for samples preparation.

As can be seen, HB plasma line has shown that the most abundant protein found in the used human plasma was around 62 kDa, also called albumin. This protein was slightly detected for all nanocapsules, but a significant difference was also observed among HES, HES-PEG and HES-PetOx proteins. It is clearly noticed the suppresion of protein adsorption on HES-PetOx 2 and 5 K surfaces when compared to HES and HES-PEG, being a strong evidence of the similar or even better stealth effect of the attached polymer PetOx. As well, the molecular weight difference among POZs may influence the shielding of the nanocapsules.

The attached proteins were also quantified using a plate reader by colorimetric standard assay. The protein amounts for HES, HES-PEG and HES-PetOx 2, 5 and 6 K are shown in Figure 8. For the non-attached HES capsules the value was 0.55 ± 0.01 mg m^{-2}, where this amount of protein decreased to 0.50 ± 0.01 mg m^{-2} for "PEGylated" HES and even more to HES-PetOx, 0.44 ± 0.02 mg m^{-2} (considering the average value among them), showing that the poly(ethyloxazoline) suppresses the protein adsorption in 10.2%, compared to 4.3% by PEG. As previously discussed, the critical property that determines the behavior of the nanocapsules under biological fluid is the stealth effect, which is directly depended on the amount and the type of bound protein on capsules' surface. Although PEG and PetOx results did not show a significant difference between them, PetOx attached on HES surface minimizes protein/surface interactions similar to PEG, exhibiting a great potential as an alternative drug delivery device to "PEGylated" systems.

Another relevant parameter is the intrinsic PetOx polymer polarity itself influences the stealth effect. We used different molecular weights of POZs that allow us to investigate how the hydrophilic-lipophilic balance of the polymer affects the protein/surface interaction of the modified capsules. Cedervall *et al.*[41] have investigated the bound-protein dependence on particle hydrophobicity and size, showing that the stoichiometry of protein/nanocapsules, i.e., the number of bound proteins *per* capsules, increase with the capsules' hydrophobicity and size.

As should be expected, for the values obtained in this work, the amount of protein adsorbed to HES-PetOx 2, 5 and 6 K on the surface of the capsules was 0.46, 0.41 and 0.44 mg m^{-2}, respectively, found to be lower than

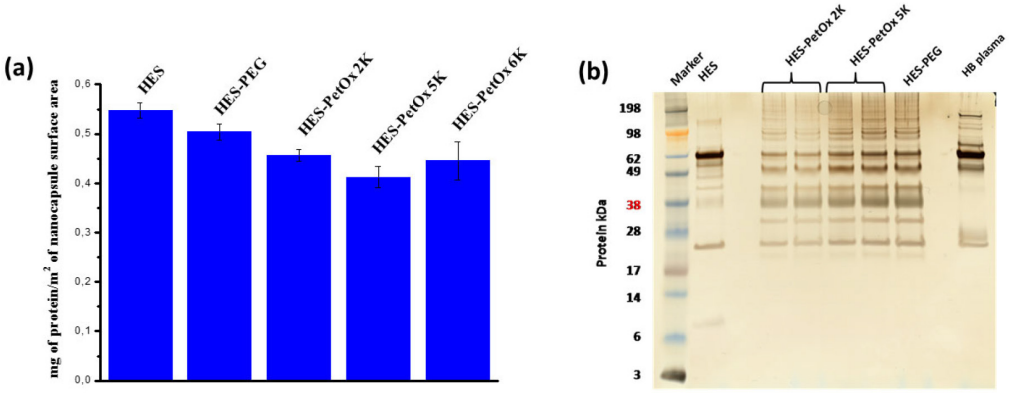

Figure 7. (a) Quantification of protein corona formed on nanocapsules surface. Left to right: HES; HES-PEG; HES-PetOx 2, 5 and 6 K; and their respectively standard deviation; and (b) SDS-PAGE gel stained with Coomassie Blue of the protein corona formed on nanocapsules surface. From left to right: protein Marker of different M_w (188-14 kDa); HES; HES-PEG as a positive control; HES-PetOx 2 and 5 K; and HB plasma as a negative control.

HES and HES-PEG. Despite our results have shown suppressed protein adsorption when capsules surface was polymer-modified, it is possible to observe a tiny difference among the obtained values for PetOx-attached HES, even considering the standard deviation (Figure 7a).

In this context, we can consider the already discussed polarity comparative study between PetOx and PEG (Figure 4c) to establish a connection between the molecular weight and chemical structure of the polymer chains and their impact on protein interactions. The results suggested that PetOx polymers become more hydrophobic increasing the molecular weight. This relatively hydrophobic behavior directly influences the hydration layer that prevents possible protein adsorption. In other words, an increase in hydrophobicity becomes strong enough to overcome the stealth effect from the polymer itself, negatively affecting the shielding of the capsule.[19] As well as observed for HES-PetOx, increasing the molecular weight of the polymer increases protein adsorption on capsules surface. Additionally, Cedervall *et al*.,[41] in a further investigation, also related the influence of different parameters from the polymer on the protein corona such as surface density, conformation and flexibility of attached polymer chains on the surface of the nanocapsules, which are not taken into discussion in this work. Thereby, our PetOx-"clicked" HES systems were efficient as much as "PEGylated" HES, which provide a versatile and satisfying protein suppressor as a potential drug delivery nanocarrier.

Protein corona composition

To deeply investigate the adsorbed proteins on polymer-modified HES nanocapsule surface, the protein corona composition was analyzed by LC-MS after plasma incubation, where a total of 20 different protein-types were identified for unmodified and polymer-modified HES nanocapsules in the so-called "hard" corona (Figure 8). The percentage of each protein was calculated from the molar mass spectrometry, considering a minimum limit amount of 1% of the total protein amount.

As can be seen in Figure 8, the heat map shows that the most abundant protein found in the "hard" corona for all analyzed nanocapsules is clusterin, an apolipoprotein found to be adsorbed to several nanocapsules/particles surface, which was also confirmed in the 38 kDa band from SDS-PAGE (Figure 7b).

Clearly, it is noticed the difference among the protein corona composition of the samples. For unmodified HES, the clusterin composes around 25-20% of the "hard" corona, while for PetOx-modified HES composes more than 35%

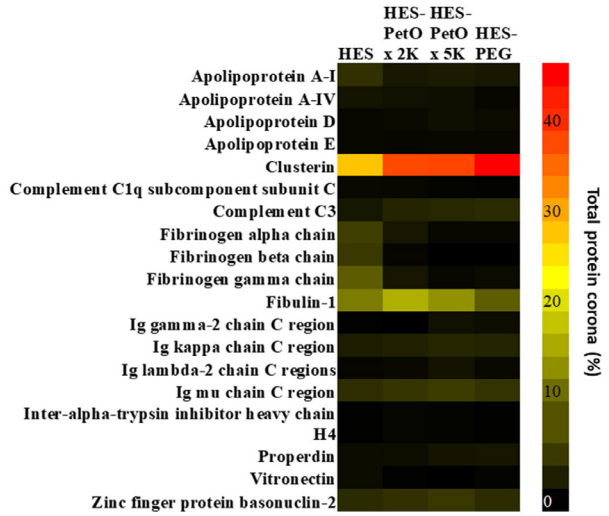

Figure 8. Heat map of proteins in the hard corona on nanocapsules surface: HES, HES-PetOx 2 K and 5 K, and HES-PEG (as a positive control) determined by LC-MS.

and even more for HES-PEG, < 40%. All other relative percentages of protein are distributed as shown in the heat map, with fibulin-1, fibrinogen, immunoglobulin C (IgC), complement C3 and zinc-2. In accordance, in previous published works,[7,9] the apolipoprotein clusterin was also reported as one of the most abundant adsorbed protein on the "hard" corona of PEG-modified polystyrene nanoparticles and sugar-modified HES nanocapsules, and even more clusterin amount has been related to polyphosphoester-modified polystyrene nanoparticles, since polyphosphoester functionalization can increase the surface hydrophobicity. In addition, some publications[7-9,42] have reported higher adsorption of apolipoproteins (as clusterin) on more hydrophobic surfaces, truly consistent, since apolipoproteins are mainly lipids.

However, as observed in our work, HES-PEG and HES-PetOx nanocapsules have shown similar protein composition profile, concerning clusterin amount, but present different polarities. Actually, HES-PEG surface slightly adsorbed more clusterin, even with PEG being more hydrophilic. According to some studies,[36,42] besides PEG is a rather hydrophilic polymer, which should adsorb mainly albumin, fibrinogen and immunoglobulin G (IgG) as more abundant proteins, apolipoproteins have different link-ways to adsorb, e.g., the adsorption is not just related to the lipid-binding interaction. For instance, clusterin has been reported to adsorb, as one of the most abundant protein, onto different kinds of nanoparticle/capsules surfaces such as silica and polystyrene nanoparticles, which clearly show distinct chemical profiles.

Since our group has been proved that clusterin can reduce around 75.4% the non-specific cellular uptake in

front of macrophage cells,[7,9] these remarkable differences in the composition of clusterin in the "hard" corona, varying different polymers, seem to drive the "stealth" effect of the nanocapsules, which should be further investigated in the presence of the immune system-cells. Nevertheless, it is noticed that the "stealth" effect is not only promoted by suppressing protein adsorption but also adsorbing a specific type of apolipoprotein.

Conclusions

This work proposed to develop a versatile protein suppressor device as an alternative to "PEGylated" nanocarrier, considering PEG non-biodegradability limitation. Within the field of polymer science, we combined both biodegradability and protein suppression of HES and PetOx with the aid of DBCO "click" chemistry, providing, in nanoscale, a suitable and satisfying protein suppressor nanocarrier. Certainly, the selected synthesis strategy, employing the interfacial polyaddition crosslinker reaction with TDI through the inverse miniemulsion technique, yielded HES nanocapsules with an aqueous core. These capsules offer opportunities for surface post-modification and feature a versatile and highly adaptable shell structure suitable for loading hydrophilic drugs. The considerable amount of primary amino groups on HES surface promoted the further PetOx modification via stable and selective triazole moiety, giving an efficiency of conversion around ca. 60%. PetOx-modified HES and unmodified HES nanocapsules were later investigated regarding the size and stability in aqueous medium, showing a capsule shell < 200 nm, even after polymer attachment, with decreasing in colloidal stability values around −30 mV, generating certain evidence of the covalently coupling and purification efficiency. GPC technique indirectly showed no physically or free adsorbed polymer traces on the surface of the capsules after purification process.

Furthermore, both protein suppression and non-aggregation behavior of HES-PetOx promoted by polymer layer were proved, concerning the outstanding success in suppressing protein adsorption and no aggregates formation into human plasma. Moreover, a fundamental study involving polarity and molecular weight of POZs was correlated with the stealth behavior of the nanocapsules, which might be an intrinsic effect from polymers chains on HES surface. We believe that further advances within this relatively new research area will help to develop POZ-based materials that fully exploit the versatility of this interesting class of polymers in biomedical applications.

Supplementary Information

Supplementary information is available free of charge at http://jbcs.sbq.org.br as PDF file.

Acknowledgments

This study was partially supported by the Coordenação de Aperfeiçoamento de Pessoal de Nível Superior - Brasil (CAPES) - Finance Code 001 (PROEX 23038.000509/2020-82), Conselho Nacional de Desenvolvimento Científico e Tecnológico (CNPq), and CAPES (L.M.U.D. Fechine). The authors thank Central Analítica UFC/CT-INFRA/MCTI-SISNANO/CAPES for the support. The corresponding author thanks CNPq for the research grant (N.M.P.S.R No. 309795/2021-4) and CAPES-PROBRAL-DAAD project, Process No. 88881.700853/2022-01.

Author Contributions

Lillian M. U. D. Fechine was responsible for investigation, formal analysis, writing original draft and editing; Biao Kang for investigation; Susanne Schöttler for investigation; Denise R. Moreira for data curation and writing-review; Danilo C. Queiroz for data curation and writing-review; Frederik R. Wurm for project administration; Katharina Landfester for conceptualization, funding acquisition, and writing-review and editing; Nágila M. P. S. Ricardo for project administration, writing-review and editing, and funding acquisition.

References

1. Sun, X.; Wang, J.; Wang, Z.; Zhu, C.; Xi, J.; Fan, L.; Han, J.; Guo, R.; *J. Colloid Interface Sci.* **2022**, *610*, 89. [Crossref]
2. Bassyouni, F.; ElHalwany, N.; Abdel Rehim, M.; Neyfeh, M.; *Res. Chem. Intermed.* **2015**, *41*, 2165. [Crossref]
3. Oliveira, S. N.; Uchoa, A. F. J.; Moreira, D. R.; Petzhold, C. L.; Weiss, C. K.; Landfester, K.; Ricardo, N. M. P. S.; *J. Braz. Chem. Soc.* **2023**, *34*, 560. [Crossref]
4. Sousa, A. C. C.; Romo, A. I. B.; Almeida, R. R.; Silva, A. C. C.; Fechine, L. M. U.; Brito, D. H. A.; Freire, R. M.; Pinheiro, D. P.; Silva, L. M. R.; Pessoa, O. D. L.; Dendardin, J. C.; Pessoa, C.; Ricardo, N. M. P. S.; *Carbohydr. Polym* **2021**, *264*, 118017. [Crossref]
5. dos Santos, S. B. F.; Pereira, S. A.; Rodrigues, F. A. M.; da Silva, A. C.; de Almeida, R. R.; Sousa, A. C. C.; Fechine, L. M. U. D.; Denardin, J. C.; Araneda, F.; Sá, L. G. A. V.; Silva, C. R.; Nobre Jr., H. V.; Ricardo, N. M. P. S.; *Int. J. Biol. Macromol.* **2020**, *164*, 2813. [Crossref]
6. Pereira, S. A.; dos Santos, S. B. F.; Rodrigues, F. A. M.;

Fechine, L. M. U. D.; Vieira, Í. G. P.; Denardin, J. C.; Araneda, F.; Ribeiro, M. E. N. P.; Gramosa, N. V.; Ricardo, N. M. P. S.; *Mater. Lett.* **2020**, *274*, 127983. [Crossref]

7. Simon, J.; Christmann, S.; Mailänder, V.; Wurm, F. R.; Landfester, K.; *Isr. J. Chem.* **2018**, *58*, 1363. [Crossref]
8. Kang, B.; Okwieka, P.; Schöttler, S.; Seifert, O.; Kontermann, R. E.; Pfizenmaier, K.; Musyanovych, A.; Meyer, R.; Diken, M.; Sahin, U.; Mailänder, V.; Wurm, F. R.; Landfester, K.; *Biomaterials* **2015**, *49*, 125. [Crossref]
9. Schöttler, S.; Becker, G.; Winzen, S.; Steinbach, T.; Mohr, K.; Landfester, K.; Mailänder, V.; Wurm, F. R.; *Nat. Nanotechnol.* **2016**, *11*, 372. [Crossref]
10. Mishra, P.; Nayak, B.; Dey, R. K.; *Asian J. Pharm. Sci*. **2016**, *11*, 337. [Crossref]
11. Suk, J. S.; Xu, Q.; Kim, N.; Hanes, J.; Ensign, L. M.; *Adv. Drug Delivery Rev.* **2015**, *99*, 28. [Crossref]
12. Li, D.; Zhao, J.; Ma, J.; Yang, H.; Zhang, X.; Cao, Y.; Liu, P.; *Colloids Surf., B* **2022**, *211*, 112330. [Crossref]
13. Reichert, C.; Borchard, G.; *J. Pharm. Sci.* **2016**, *105*, 386. [Crossref]
14. Floris, P.; Garbujo, S.; Rolla, G.; Giustra, M.; Salvioni, L.; Catelani, T.; Colombo, M.; Mantecca, R.; Fiandra, L.; *Nanomaterials* **2021**, *11*, 1004. [Crossref]
15. Wang, W.; Zhang, L.; Le, Y.; Chen, J. F.; Wang, J.; Yun, J.; *Int. J. Pharm*. **2016**, *498*, 134. [Crossref]
16. Ulbricht, J.; Jordan, R.; Luxenhofer, R.; *Biomaterials* **2014**, *35*, 4848. [Crossref]
17. Garay, R. P.; El-Gewely, R.; Armstrong, J. K.; Garratty, G.; Richette, P.; *Expert Opin. Drug Delivery* **2012**, *9*, 1319. [Crossref]
18. Verhoef, J. J. F.; Anchordoquy, T. J.; *Drug Delivery Transl. Res*. **2013**, *3*, 499. [Crossref]
19. Viegas, T. X.; Bentley, M. D.; Harris, J. M.; Fang, Z.; Yoon, K.; Dizman, B.; Weimer, R.; Mero, A.; Pasut, G.; Veronese, F. M.; *Bioconjugate Chem.* **2011**, *22*, 976. [Crossref]
20. Adams, N.; Schubert, U. S.; *Adv. Drug Delivery Rev*. **2007**, *59*, 1504. [Crossref]
21. Sedlacek, O.; de la Rosa, V. R.; Hoogenboom, R.; *Eur. Polym. J.* **2019**, *120*, 109246. [Crossref]
22. Varanaraja, Z.; Kim, J.; Becer, C. R.; *Eur. Polym. J.* **2021**, *147*, 110299. [Crossref]
23. Goossens, H.; Catak, S.; Glassner, M.; de la Rosa, V. R.; Monnery, B. D.; De Proft, F.; Speybroeck, V. V.; Hoogenboom, R.; *ACS Macro Lett.* **2013**, *2*, 651. [Crossref]
24. Makino, A.; Kobayashi, S.; *J. Polym. Sci., Part A: Polym. Chem*. **2010**, *48*, 1251. [Crossref]
25. Luxenhofer, R.; Sahay, G.; Schulz, A.; Alakhova, D.; Bronich, T. K.; Jordan, R.; Kabanov, A. V.; *J. Controlled Release*. **2011**, *153*, 73. [Crossref]
26. Tauhardt, L.; Kempe, K.; Gottschaldt, M.; Schubert, U. S.; *Chem. Soc. Rev.* **2013**, *42*, 7998. [Crossref]
27. Lava, K.; Verbraeken, B.; Hoogenboom, R.; *Eur. Polym. J.* **2015**, *65*, 98. [Crossref]
28. Crespy, D.; Landfester, K.; *Beilstein J. Org. Chem.* **2010**, *6*, 1132. [Crossref]
29. Landfester, K.; Mailander, V.; *Expert Opin. Drug Delivery* **2013**, *10*, 593. [Crossref]
30. Hein, C. D.; Liu, X.-M.; Wang, D.; *Pharm. Res.* **2008**, *25*, 2216. [Crossref]
31. Tron, G. C.; Pirali, T.; Billington, R. A.; Canonico, P. L.; Sorba, G.; Genazzani, A. A.; *Med. Res. Rev.* **2008**, *28*, 278. [Crossref]
32. Baier, G.; Siebert, J. M.; Landfester, K.; Musyanovych, A.; *Macromolecules* **2012**, *45*, 3419. [Crossref]
33. Voigt, M.; Fritz, T.; Worm, M.; Frey, H.; Helm, M. In *Pharmaceutical Nanotechnology* Volkmar Weissig, V.; Elbayoumi, T., eds.; Humana Press: New York, USA, 2019, p. 235. [Crossref]
34. Böhlen, P.; Stein, S.; Dairman, W.; Udenfriend, S.; *Arch. Biochem. Biophys.* **1973**, *155*, 213. [Crossref]
35. Rausch, K.; Reuter, A.; Fischer, K.; Schmidt, M.; *Biomacromolecules* **2010**, *11*, 2836. [Crossref]
36. Tenzer, S.; Docter, D.; Rosfa, S.; Wlodarski, A.; Kuharev, J.; Rekik, A.; Knauer, S. K.; Bantz, C.; Nawroth, T.; Bier, C.; Sirirattanapan, J.; Mann, W.; Treuel, L.; Reinhard Zellner, R.; Maskos, M.; Schild, H.; Stauber, R. H.; *ACS Nano* **2011**, *5*, 7155. [Crossref]
37. Landfester, K.; *Angew. Chem., Int. Ed.* **2009**, *48*, 4488. [Crossref]
38. Eslahian, K. A.; Lang, T.; Bantz, C.; Keller, R.; Sperling, R.; Docter, D.; Stauber, R.; Maskos, M. In *Measuring Biological Impacts of Nanomaterials*, vol. 5; Wegener, J., ed.; Springer: Cham, 2014. [Crossref]
39. Agard, N. J.; Baskin, J. M.; Prescher, J. A.; Lo, A.; Bertozzi, C. R.; *ACS Chem. Biol.* **2006**, *1*, 644. [Crossref]
40. Owens III, D. E.; Peppas, N. A.; *Int. J. Pharm.* **2006**, *307*, 93. [Crossref]
41. Cedervall, T.; Lynch, I.; Lindman, S.; Berggård, T.; Thulin, E.; Nilsson, H.; Dawson, K. A.; Linse, S.; *Proc. Natl. Acad. Sci.* **2007**, *104*, 2050. [Crossref]
42. Ritz, S.; Schöttler, S.; Kotman, N.; Baier, G.; Musyanovych, A.; Kuharev, J.; Landfester, K.; Schild, H.; Jahn, O.; Tenzer, S.; Mailänder, V.; *Biomacromolecules* **2015**, *16*, 1311. [Crossref]

Submitted: November 23, 2023
Published online: February 8, 2024